

# Fault Segmentation, Fracture Networks and Fold Development in the Western Katrol Hill Fault, Central Mainland Kachchh

Babulal Vaghela<sup>1,2\*</sup>, Chirag Jani<sup>3</sup>, Gaurav Chauhan<sup>1</sup>, Chirag Parmar<sup>1</sup>, Ishaan Parmar<sup>1</sup>, Mahesh Thakkar<sup>4</sup>, Darshit Padia<sup>2</sup>

<sup>1</sup>Department of Geoscience, KSKV Kachchh University, Bhuj, India

<sup>2</sup>Department of Geology, R. R. Lalan College, Bhuj, India

<sup>3</sup>Oil and Natural Gas Corporation Limited, Ahmedabad, India

<sup>4</sup>Birbal Sahni Institute of Palaeosciences, Lucknow, India

Email: \*mukesh77foru@gmail.com

**How to cite this paper:** Vaghela, B., Jani, C., Chauhan, G., Parmar, C., Parmar, I., Thakkar, M. and Padia, D. (2026) Fault Segmentation, Fracture Networks and Fold Development in the Western Katrol Hill Fault, Central Mainland Kachchh. *Open Journal of Geology*, 16, 139-156. <https://doi.org/10.4236/ojg.2026.163008>

**Received:** February 26, 2026

**Accepted:** March 22, 2026

**Published:** March 25, 2026

Copyright © 2026 by author(s) and Scientific Research Publishing Inc. This work is licensed under the Creative Commons Attribution International License (CC BY 4.0).

<http://creativecommons.org/licenses/by/4.0/>



Open Access

---

## Abstract

This study presents a detailed structural and fracture analysis of the western segment of the Katrol Hill Fault (KHF) and its surrounding region within the Kachchh Rift Basin in western India. Through the application of integrated geological and structural mapping, remote sensing, field investigations and paleostress analysis, this study identifies a complex fault system, oriented east-west to ENE-WSW/ESE-WNW. This system is characterized by asymmetric flexures and a network of strike-slip and oblique-slip faults. Multiple fracture types, including extension joints, veins, en-echelon shear fractures and pinnet joints, reflect successive deformation phases under evolving transtensive stress regimes oriented from N-S to NNE-SSW, influenced by magmatic intrusions such as the Nanamo Hill plug and fault activity. Fault-related folds exhibit both normal and reverse drag styles, governed by heterogeneous displacement fields along faults, with conical drag folds and brecciation, indicating mechanical heterogeneity within lithologies. The integration of field data, remote sensing and paleostress reconstruction elucidates the kinematic evolution, fault segmentation and fracture network development in the Kachchh Rift Basin, providing valuable insights into seismic hazard assessment and regional tectonic interpretations.

## Keywords

Katrol Hill Fault, Drag Fold, Fractures

---

## 1. Introduction

Deformation zones are complex systems in which fractures, faults and joints interact to control fluid flow, mechanical behavior and seismic activity [1]. Understanding these interactions is crucial for assessing seismic hazards, predicting fluid pathways and evaluating the potential for fault reactivation in various geological settings [2]-[4]. Fracture analysis involves studying the characteristics, patterns and interactions of fractures in rock formations, which includes: 1) Identifying different types of fractures (e.g., extension, compressional and shearing-mode fractures), 2) Analyzing the geometric and topological relationships between fractures, 3) Determining the relative ages of fractures, 4) Examining kinematic relationships and displacement patterns. Characterizing fracture networks and their properties [5].

The Kachchh Rift Basin (KRB) in western India is a structurally controlled basin with numerous intrabasinal faults and associated transverse faults [6] [7]. Several studies have been conducted on various aspects of the structural analysis of intrabasinal faults and associated transverse faults of the KRB [8]-[18]. These efforts have improved our knowledge of the nature and neotectonic behavior of Kachchh's intrabasinal and transverse faults.

With regard to the understanding of the stress pattern along the fault system of the KRB, most research has been conducted in the Kachchh Mainland Uplift (KMU), Wagad Uplift (WU) and Island Belt Uplift (IBU) regions [14]-[17] [19] [20] with only a few attempts at the structural and tectonic analysis of the Katrol Hill Fault (KHF) has been achieved. The first attempt was made by [12] [19]-[22] who studied fracture systems and fault systems around the Bhuj and KHF, Kachchh Mainland Fault (KMF), IBF and VGKF. In addition, quaternary studies along the KHF are available, which describes the climate, geomorphology, morphotectonics and neotectonics aspects [10] [11] [23]-[31]. This provided basic information on the orientation of regional fractures, their possible origin and their neotectonic and activation in the Quaternary period. As for the fracture morphology, the time relation and other criteria of fracture in different formations of rocks remain a question. This study aims to understand the various joints, faults, fault-related folds and their relationship to outcrop and regional-scale deformation in the western segment of the KHF.

## 2. Location and Geology of the Study Area

The study area is located in the central Kachchh mainland of the Kachchh region (Figure 1) and consists of the Charwar hill Uplift along the western part of the KHF, starting from the West of Deshalpar village to Varamseda in the west. The study area is bounded by the Bhuj low in the north and the Dhola hill range in the south.

### 2.1. Stratigraphy

The study area represents Mesozoic rock of the Jhuran and Bhuj formations and

a thin cover of Quaternary Alluvium [21] [32]. Jhuran Formation in the Charwar Range is uniform and comparable to the type section [21] [32]. The formation's thickness varies between 1000 and 1370 ft. and is sporadically fossiliferous [21] [32]. The study area is mostly outcropped by the Bhuj formation starting from Kurbai village, represented by the Kurbai Plant Bed, a dark carbonaceous shale (8 - 10 ft. thick), containing rich plant fossils and later surrounding the outcrops of the Jhuran formation [21]. The Bhuj Formation surrounding Jhuran is represented by the intercalation of sandstone siltstone shale beds and massive sandstone beds of the lower members of the Bhuj Formation [21] [32].

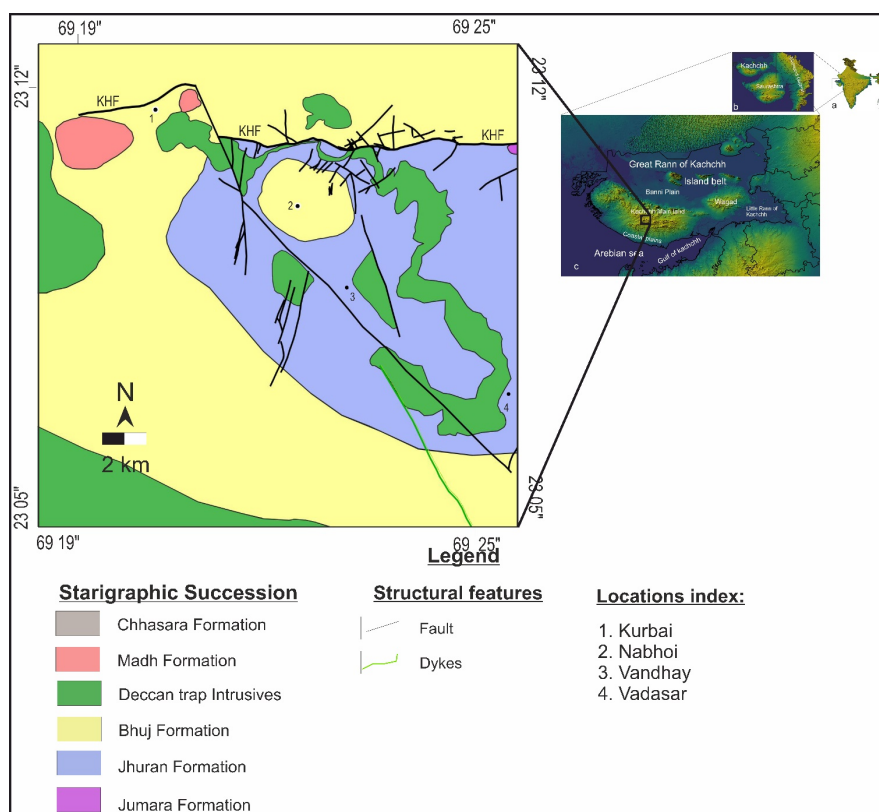


**Figure 1.** Location and geological map of the study area with major lithologies and structures [7].

## 2.2. Structure

The structural features of the western part of the Charwar Range flexure are characterized by a marginal long narrow anticline along the KHF and a second, sub-parallel to the oblique axis of folding to its south [7] [8] [21] (Figure 2). The western part of the marginal anticline includes the Gurukul Dungar Anticline, Dhru-biya Half Anticline and Waramseda Plunging Syncline. A prominent structural basin, the Kurbai Basin, is located in the low area between the Gurukul anticline, Dhru-biya half-dome and Waramseda nose [21]. The marginal anticline of the KHF terminates in a sharp nose near Waramseda, west of the Dhru-biya half-dome [7] [21]. South of the Kurbai Basin lies a fold axis parallel to the Nabhoi fault, a

prominent fault with a length of 13 km, which shows three different fold structures along the trace.

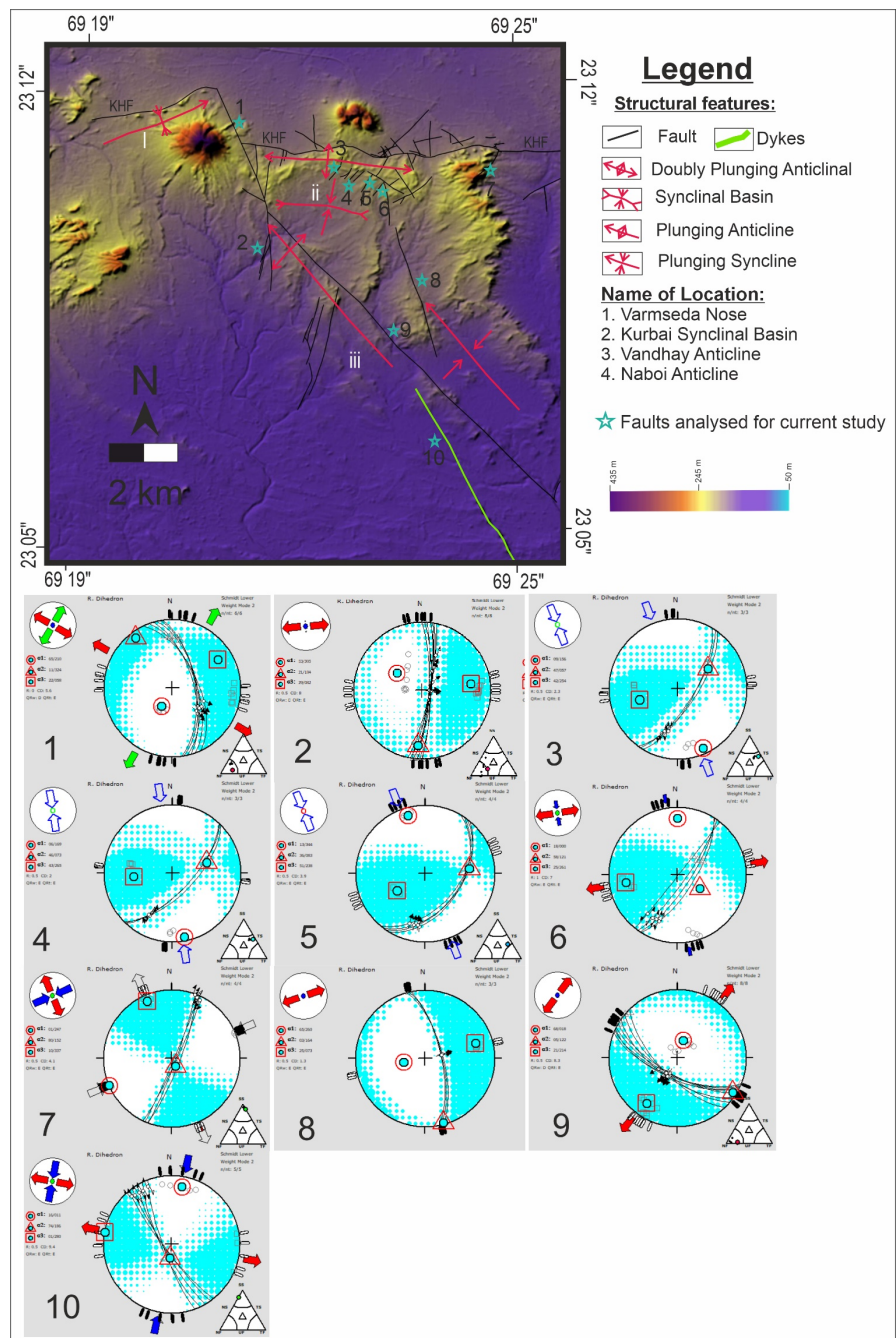


**Figure 2.** Structural map of the study area on a 30 m resolution DEM with major fold axis, faults with stereograms, PBT axis and stress directions [7].

Igneous activity was more pronounced in the western region. Large plutons, such as the Nanamo Hill Plug south of Varmseda and Mangwana, invade the marginal folds [7] [21] [33]. A very large sill starting from the Dhrubiya half-dome defines folds, as it outcrops from the north to the south of the study area [21] [33].

Apart from a few dykes near the Nanamo Hill plug, a transverse dyke originating from Deccan trap rocks crosses the Sill.

### 3. Methodology

#### 3.1. Structural and Geological Mapping

The methodology involves geological and structural mapping of the study area, as well as the analysis of fault-related folds using a combination of remote sensing, field data collection and analytical techniques.

Fault data and fold boundaries were digitized from published maps using GIS software. Satellite imagery and Google Earth Pro (GEP) map major structures, lineaments and folds, which are overlaid on a 30 m Copernicus Global Digital Elevation Model. Google Earth Pro was used to identify lineaments on the anticlines and measure their orientation and length. Remote sensing techniques, including directional filtering, overlaying of lithological units and extraction of tectonic lineaments, were further verified with field data [34].

#### Field Data Collection

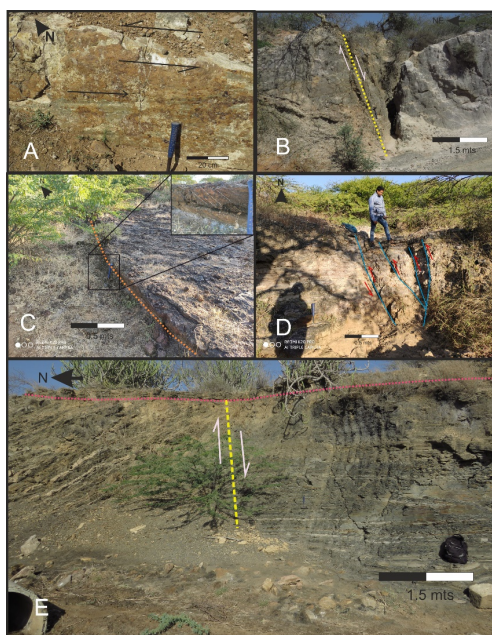


**Figure 3.** (A) Jamthada dyke plane exposing the slicken lines along the strike of the plane; (B) South-dipping fault plane of the Nabhoi fault near the Rukmavati river section south of Vadasar Village; (C) A Sinistral reverse fault with slicken lines near Kurbai Madhpar road indicates a reverse oblique slip movement in the NW direction; (D) Sinistral reverse Fault zone with Positive flower structure along a narrow river valley East of Kurbai village; (E) Nabhoi fault with dipping bed on NE (up thrown block) and horizontal on SW (down thrown block) exposed in a river SE of Nabhoi village.

Fieldwork was conducted in the exposed sections of fault and fold limbs in the vicinity of the western segment of the KHF. Clear photographs of the fault planes were captured. Ten faults and folds along them were selected for the present study

and various elements and structural features were measured on selected sites for structural analysis. The fault data include the azimuth of the fault planes, dip direction, dip amount, and kinematic indicators along the slickenside surfaces, such as the rake and plunge of the slickenlines (**Figure 3**). Multiple data points were collected from a single fault plane at different locations along the same fault to minimize errors and to address any variability in kinematics along the fault plane, if present. Data pertaining to the fold-limbs was collected for the purpose of drag fold analysis. Additionally, data concerning various joint sets were documented (**Figure 4**). The dataset includes types of joint, mineralization present, orientation, and its relationship with lithology and major structural features in the surrounding area.

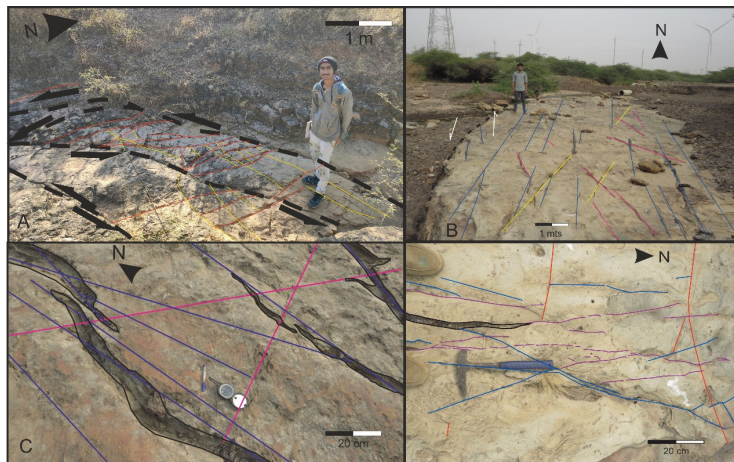


**Figure 4.** (A) Sinistral reverse fault zone with a positive flower structure along a narrow river valley East of Kurbai village. Note the small reverse faults along with the pinnet joints and younger joints crossing the faults; (B) A dextral normal fault across the river, with I, Y and X open mode joints and open en-echelon joints; (C) Various types of fractures are represented by sealed joints, open-mode en-echelon joints parallel to sealed joints and joints forming limonitic box works; (D) Joints along with an en-echelon calcite vein between the hammer and the open joint (**Blue:** N-S, **Yellow:** NE-SW, **Purple:** NW-SE, **Pink:** E-W).

### 3.2. Structural Analysis

Structural analysis involved the characterization of folds and faults in the study area. Detailed field work was conducted to measure the parameters for fold characterization, such as dip, strike and dip amount of the beds along the folded surface. Fault studies were conducted by measuring the dip, strike and dip amount of the faults. To conduct a paleostress analysis of the faults, the rake and pitch of the slickenlines, which are grooves on the fault surface, were measured.

#### 3.2.1. Fault-Related Fold Study

The study of fault-related folds (including drag faults and fault-bend folds) involves several key methods, including examining small-scale drag folds along faults to document their geometry and relationship to the main fault. The geometric relationships between small-scale fractures (meso-fractures) and larger faults

were observed. Identifying structures, such as faults, to determine stress or strain trajectories. Poles to bedding were plotted on stereograms to understand the overall geometry of the folds (e.g., conical or cylindrical). These field studies allow a detailed description of fault segmentation, fault-related fold architecture at various evolutionary stages and the relationship between folding and lithological units (members).

The asymmetry and vergence of the folds were analyzed in relation to the fault orientation and slip direction. For fault-bend folds, documenting the changes in the dip of the fault surface and the corresponding changes in fold geometry is a key aspect and by integrating these methods, a genetic relationship between the faults and their associated folds can be established to interpret the broader deformation history of the region.

### 3.2.2. Paleostress Analysis

Paleostress analysis involves the calculation of stresses incurred during a deformation event in a region or body [35]. Paleo-stresses are indicated by stress tensors consisting of three mutually perpendicular principal axes along tectonic zones [35]-[37]. The measurement of fault plane orientations and slickenside striations is crucial for determining the slip directions [36]. Surface markings on faults, such as striations and steps, provide vital information regarding fault movement and stress orientation.

Win Tensor is a paleostress reconstruction program developed by Damien Delvaux initially for DOS and later converted to Windows. The version of the program used was Win Tensor 5.9, which was developed in 2021. The methods available for constructing stress tensors are the PBT axis method and the Right Dihedra Method (RDM) [35]. The fault inversion analysis also generates three strain axes,  $\sigma_1$  (maximum),  $\sigma_2$  (intermediate) and  $\sigma_3$  (minimum); and their orientation in the tensors. The calculated stress ratio is essential for defining the stress regime of the fault plane slip data. The stress regime is calculated under three defined criteria: 1) when  $\sigma_1$  is vertical, it defines an extensional regime under which  $R' = R$ , which is further sub-divided into radial extensive ( $R' = 0 - 0.25$ ), pure extensive ( $R' = 0.25 - 0.75$ ) and transtensive ( $R' = 0.75 - 1.25$ ); 2) when  $\sigma_2$  is vertical, it defines a strike-slip regime under which  $R' = 2 - R$ , which is further sub-divided into pure strike-slip ( $R' = 1.25 - 1.75$ ) and transpressive ( $R' = 1.75 - 2.25$ ); when  $\sigma_3$  is vertical, it defines compressive regime under which  $R' = 2 + R$ , which is further sub-divided into pure compressive ( $R' = 2.25 - 2.75$ ) and radial compressive ( $R' = 2.75 - 3.0$ ) regime [37].

## 4. Field Investigation and Data Analysis

The study area represents the westernmost part of the KHF and consists of various generations of faults and folds. The KHF is generally an east-west trending fault with an occasional change in the trend of the fault strike to ENE-WSW to ESE-WNW. It has produced a narrow Flexure (150 - 200 m width) parallel to the fault. The northern flank of the flexure is mostly eroded, with a few outcrops preserved

along with the exposed KHF. The southern flank is abrupt and parallel to the KHF, which is further dissected by several crisscross-cutting transverse faults [7] [8]. The flexures along the southern flank are moderate-dipping asymmetric folds with an average dip of  $35^\circ$  towards the KHF and  $15^\circ - 20^\circ$  away from the KHF towards the south.

The Flexure is dissected by many faults with strikes Perpendicular or Oblique to KHF (Figure 2). The data of faults determine it to be strike-slip and oblique-slip in nature and at places, they dissect and displace the KHF. In the western part between Magwana and Varamseda village, a subsidiary NNW-SSE fault with a dip of  $64^\circ$  towards the East divides the KHF into two parts, forming the Varamseda nose in the north-west region. Field evidence and fault data suggest that this fault is transtensive (Stereogram 1 of Figure 2). The contact between this subsidiary fault and the KHF forms the Varamseda syncline (Figure 5(D)), which appears to be a noncylindrical plunging drag fold created during the faulting of the KHF and subsidiary fault.

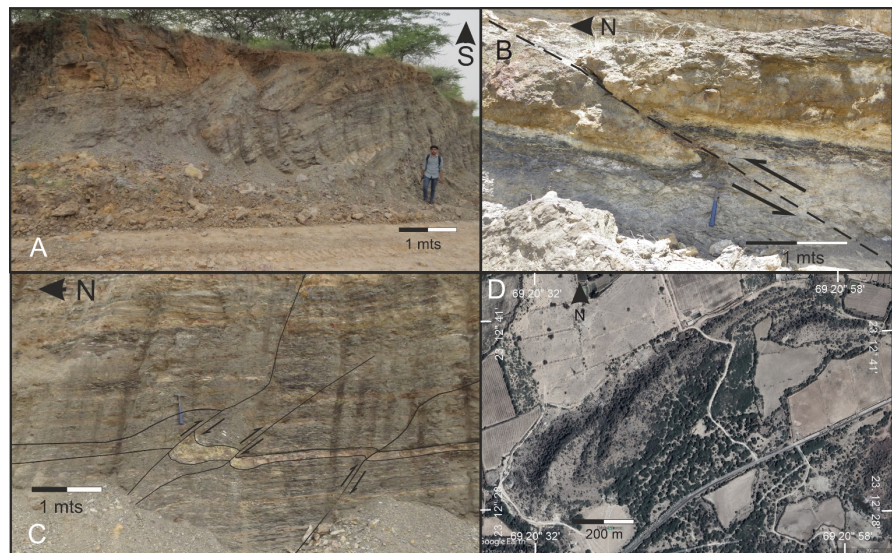


**Figure 5.** (A) NW limb of the Nabhoi anticline along the Nabhoi Fold; (B) A low-angle reverse fault section with normal drag in shale sandstone intercalation of the Bhuj formation, Rukmavati river, south of Vadasar; (C) A series of low-angle reverse faults with normal drag along the fault plane in the Black Shales of Jhuran formation, 2 km east of Mangwana Gadhashisa road; (D) Google Earth view of Varamseda Plunging Non-Cylindrical Syncline dipping ENE to NE.

This fault is large compared to other faults near the KHF and extends 7 km SE, dissecting and cross-cutting the Nanamo Hill plug, Dhrubiya Sill and Nabhoi fault. Near the SE end of the fault, it merges with three to four high-angle en-echelon normal and sinistral strike-slip faults. The sandstone of the Jhuran formation shows various types of fractures, including calcite veins oriented in the N-S (purple colour line in Figure 4(B)), box work fractures and orthogonal joint sets oriented in the N-S, E-W, NW-SE and NE-SW directions (Figures 4(B)-(D)) and an

open-mode en-echelon shear fracture system (**Figures 4(B)-(D)**). These en-echelon fractures show signs of tearing and faulting in the presence of transtensive stress.

On the northern side near the north limb of the Kurbai synclinal basin, a series of en-echelon dextral oblique slip faults crosscut the Jhuran and Bhuj formation rocks (**Figure 1**). The throw of these faults varies from a few meters to a few tens of meters. **Figure 3(C)** and **Figure 3(D)** show two such faults from Sites 5 and 6, respectively. Both these faults are oblique slip faults (reverse dextral faults) and the fault at site 6 shows a positive flower structure. These faults cross the Dhrubiya half dome and other parts of the flexure near the KHF. The fault at site 6 shows pinnate joints and an array of en-echelon faults and joints developed within the fault zone (**Figure 4(A)**). All these faults are transpressive in nature with maximum compression from NNW-SSE and NW-SE (stereograms of site 3, 4, 5 and 6 in **Figure 2**).

The flexure formed north of Kurbai village by the KHF shows several types of fractures, including orthogonal strike joints, dip joints and cross joints oblique to flexure (**Figure 6(A)** and **Figure 6(B)**). The orientation of these joints and faults is mainly N-S, E-W, NE-SW and a few NW-SE. Strike and dip joints appear to be formed by expansion during flexural folding on different flanks.

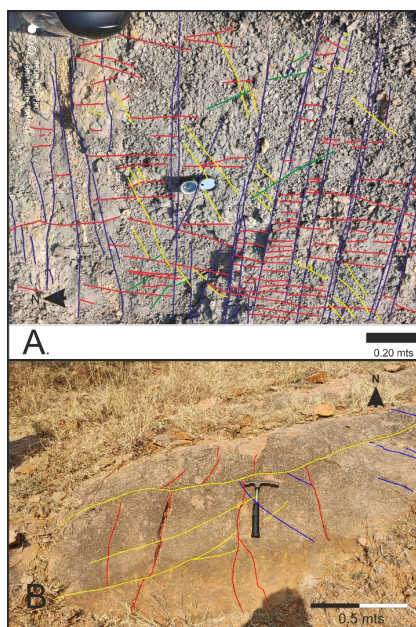


**Figure 6.** (A) Jhuran Shale showing orthogonal joint sets with various abutting relationships and I, Y, and X nodes; (B) Jhuran sandstone with open mode N-S joints and NW-SE, NE-SW cross joints (**Red:** N-S, **Yellow:** NE-SW, **Green:** NW-SE, **Blue:** E-W).

In the eastern part near the Gurukul Dungar anticline, a NE-SW fault at site 6 (**Figure 1** and **Figure 2**) crosses the Jhuran Formation across the anticline and displaces the KHF by several tens of meters. This fault shows a typical strike-slip movement, which can be observed by the formation of overturned anticlines and

small horizontal flexures near the fault in the Jhuran rocks, indicating a pure strike-slip stress pattern (stereogram 7 in **Figure 2**).

The major feature of the southern part is a 12 km long NW-SE striking Nabhoi fault, which is a normal fault dipping south at an angle of 64° - 68°. The fault is exposed in the Vadasar River section, a tributary of the Rukmavati River. Analysis of the Nabhoi fault plane data suggests a pure extensive stress in the NE-SW direction. The fault plane forms an anticline plunging NW on the downthrown block in the NW tip of the fault (**Figure 5(A)**). A second structure in the form of a NW-plunging synclinal basin is observed near the NE of Nabhoi village, which is large and broad compared to the anticline in the NW. Apart from this, the southern side of the study area shows low-angle reverse faults with very minor displacement. However, despite their small scale, these faults indicate the formation of drag folds along their displacement (**Figure 5(B)** and **Figure 5(C)**).

**Table 1.** Fault data with a sense of slip Lithology, Stress axis, Shmax, Shmin, Regime Index (RI) and stress regime. (NS: Pure Extensive [37], TS: Transpressive [37], NF: Transtensive [37]. SS: Pure Strike-Slip [37]. UNF: Unnamed Fault, ND: Normal Dextral, NS: Normal Sinistral, IS: Inverse/Reverse Sinistral, ID: Inverse/Reverse Dextral.

| Site | Fault name    | Sense of Slip | Lithology    | No. of Collected fault data | $\sigma_1$      | $\sigma_2$      | $\sigma_3$      | Map parameters |       |     |               |
|------|---------------|---------------|--------------|-----------------------------|-----------------|-----------------|-----------------|----------------|-------|-----|---------------|
|      |               |               |              |                             |                 |                 |                 | Shmax          | Shmin | RI  | Stress regime |
| 1    | UNF           | ND            | Bhuj, Jhuran | 8                           | 217 $\angle$ 61 | 011 $\angle$ 26 | 106 $\angle$ 11 | 020            | 110   | 0.5 | NF            |
| 2    | UNF           | NS            | Jhuran       | 8                           | 339 $\angle$ 43 | 183 $\angle$ 45 | 081 $\angle$ 12 | 166            | 076   | 0.5 | NF            |
| 3    | UNF           | IS            | Bhuj         | 3                           | 164 $\angle$ 21 | 051 $\angle$ 45 | 271 $\angle$ 37 | 171            | 081   | 2.0 | TS            |
| 4    | UNF           | IS            | Bhuj         | 3                           | 179 $\angle$ 18 | 069 $\angle$ 47 | 283 $\angle$ 38 | 005            | 095   | 20  | TS            |
| 5    | UNF           | IS            | Bhuj, Jhuran | 4                           | 338 $\angle$ 13 | 078 $\angle$ 36 | 232 $\angle$ 51 | 153            | 063   | 2.0 | TS            |
| 6    | UNF           | IS            | Bhuj, Jhuran | 4                           | 160 $\angle$ 05 | 063 $\angle$ 55 | 254 $\angle$ 35 | 161            | 071   | 1.5 | SS            |
| 7    | UNF           | ID            | Jhuran       | 4                           | 245 $\angle$ 03 | 121 $\angle$ 85 | 335 $\angle$ 04 | 065            | 155   | 1.5 | SS            |
| 8    | UNF           | N             | Bhuj         | 3                           | 258 $\angle$ 64 | 348 $\angle$ 00 | 078 $\angle$ 26 | 168            | 078   | 0.5 | NF            |
| 9    | Nabhoi Fault  | N             | Bhuj, Jhuran | 10                          | 022 $\angle$ 68 | 112 $\angle$ 00 | 202 $\angle$ 22 | 112            | 022   | 0.5 | NS            |
| 10   | Jamthada Dyke | ND            | Bhuj         | 5                           | 076 $\angle$ 24 | 204 $\angle$ 76 | 114 $\angle$ 00 | 009            | 099   | 1.5 | SS            |

The Jamthada dyke, named after the village Jamthada, crosscuts the Dhruviya sill (**Figure 1**). The dyke serves as site 10, which is located South of the Nabhoi fault and has a NW-SE trend. The dyke shows slicken lines parallel to the strike, indicating later reactivation of the fault along the intrusion, which is dextral strike-slip in nature (**Figure 3(A)**). This indicates a transition of stress from pure extensive to pure strike-slip in (Stereogram 10 in **Figure 2**). Outcrops and remote sensing imagery show no sign of dykes crosscutting the Nabhoi fault. Site 8 shows another such feature located NE of the Nabhoi village. A normal fault with a NW-SE strike has formed a fault scarp with the outcrops of the Dhruviya sill in the SW (**Figure 1** and **Figure 2**). This fault has a length of nearly 4 km with a down throw in the NE direction, although the nature of this fault is in question as it may be an

oblique slip or strike-slip fault as good exposure of the fault plane with slickens are not available. **Table 1** shows the fault data of the study area with their PBT or  $\sigma_1$ ,  $\sigma_2$  and  $\sigma_3$  axis.

## 5. Relationship between Faults and Other Fractures

The study of mesofractures, such as small faults, veins and joints, is a powerful tool for determining regional stress and strain trajectories [38]. The fractures in the study area are represented by various types of faults, joints and veins. [39] describes the temporal relationships between various joints and faults. Even a single joint set often shows evidence of development through a multi-phase failure sequence. By stating this, [38] implies that tectonic stress fields are not static and that rock masses are progressively fractured over time. This can be seen as the N-S joint system prevailing in the study area, but at the same time, it is made up of different kinds of fractures, such as open mode extension fractures, veins and sealed joints. This indicates that all joints with this orientation were formed during different deformation events.

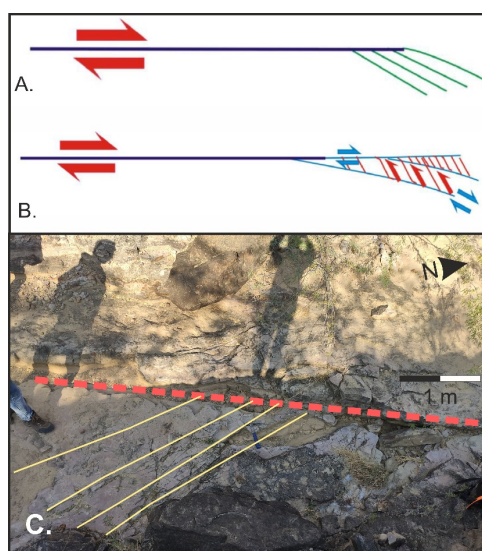


**Figure 7.** (A) Strike-slip fault with pinnate fractures or horse tails; (B) Reactivation of these joints forms antithetic faults (modified from [1]); (C) Pinnate joints in the strike slip fault in a narrow river valley East of Kurbai village (See **Figure 4(A)** for similar features in same fault).

Most faults in the study area are oblique slip faults, either reverse or normal oblique faults and some are normal or strike-slip faults. Fault analysis suggests that the paleo-stress conditions in the study area changed over time, during which various faults were generated or reactivated. The fault data analysis suggests N-S to NNE-SSW Transpressive stress along the Western NNE-SSW. This might have formed during the intrusion of the Nanamo Hill plug and KHF. Other faults near the KHF show a similar nature, but they appear to be reactivated. This is indicated by the nearly same orientation of the different stress patterns of compressive or

transpressive nature along the fault plane.

On the other hand, the Nabhoi fault in the south of the study area is older or synchronous to the other faults in the study area. It shows a normal or pure extensive stress field with minor variations to transtensive at a few places. This fault is crosscut and displaced by the NNE-SSE fault and shows a trailing pinnet fracture in the flexural fold of the Nabhoi fault (Site 1 Fault in **Figure 2** and **Figure 7(A)**). These trailing fractures are reactivated as faults with similar stress fields [1]. Similar pinnet joints and faults are also present in the site 6 fault (**Figure 4(A)**, **Figure 7(B)** and **Figure 7(C)**) along a narrow river valley East of Kurbai village.

## 6. Fault-Related Folds

In the study area, fault-related folds are mainly found along the KHF and Nabhoi Faults. However, these folds were modified by en-echelon faults. The KHF shows both types of drag folds in the flexure, normal drag, and reverse drag (**Figure 8**). [40] shows that the formation of either normal or reverse drag is a result of the heterogeneous displacement field created by the fault slip. This field has two main components.

1) Fault-Parallel Displacement ( $u_x$ ): This component causes a marker to bend into a concave shape in the direction of the slip, contributing to the reverse drag.

2) Fault-Normal Displacement ( $u_y$ ): This component causes the marker to bend into a convex shape in the direction of the slip, contributing to the normal drag.

Whether normal or reverse drag ultimately forms depend on which of these displacement components has a dominant effect. This dominance is determined by the orientation of the marker relative to the faults. This can be seen in the case of the nabhoi fault, a high-angle normal fault with reverse drag forming a gentle cylindrical (later Converted in Conical drag) anticline on the hanging wall and a Gentle Synclinal basin on the footwall. [40] [41] demonstrate that drag effects can change along a single fault, transitioning from reverse drag at its centre to normal drag at its termination. This seems to be true for the KHF, which shows both types of drag (**Figure 8(A)** and **Figure 8(C)**). Although more studies required for a complete understanding of the drag folds in the KHF.

The western side of the Nabhoi fault shows a NW-plunging anticline (**Figure 8(C)**). According to [42], conical drag folds are formed through the passive rotation of a competent (hard) rock bed that is surrounded by incompetent (soft), flowing media, especially in the vicinity of faults where the shear is oblique. This seems true for the above-mentioned anticline, which might have formed because of the Intersection of Nabhoi fault and NNW-SSW fault in the western part of the study area. Rocks in this particular part are represented by shale sandstone intercalations of Jhuran formation and a sill. On the SE end of the fault, a plunging syncline is observed east of the Nabhoi village and north of the Ajapar village, where an NW-SE fault crosses the syncline (**Figure 8(B)**).

The formation of conical drag folds can involve the development of small-scale faults or fractures within the competent (harder) rock layer, which causes ductile

flow and brecciation in incompetent rocks such as shale (**Figure 5(C)**) [42].

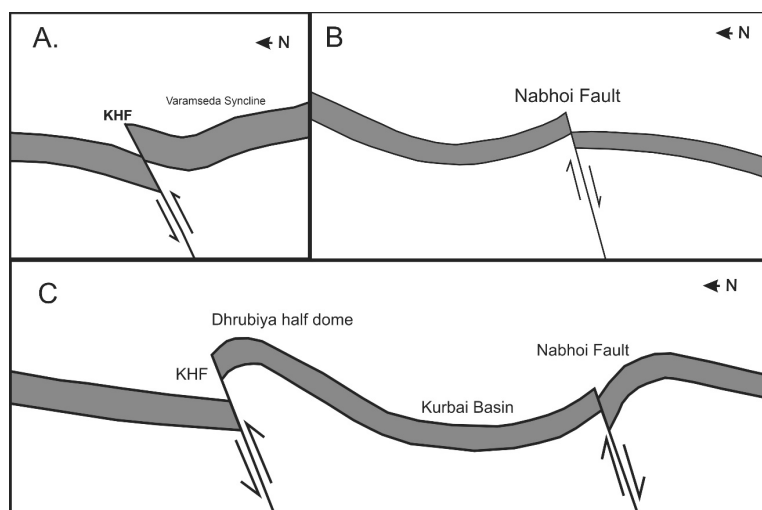


**Figure 8.** (A) A schematic section diagram for Varamseda Syncline indicating Reverse Drag Reverse fault; (B) A schematic section through SE portion of Nabhoi fault forms a syncline on the footwall indicating a reverse drag in Normal fault; (C) A schematic section diagram illustrating the normal drag in Reverse fault (KHF) forming the Dhrubiya half dome and Reverse drag in normal fault (Nabhoi fault) and formation of the Kurbai structural basin (Sections not to scale).

All these fault-related folds form a structural basin between the Nabhoi and KHF faults, Waramseda nose and Gurukul dunger anticline [21]. This was later filled by sediments eroded from the Jhuran formation black shales and deposited in the basin, forming the Kurbai plant bed, which was later gently folded due to the progressive deformation of the KHF.

## 7. Deformation History

The western segment of the Katrol Hill Fault (KHF) can be divided into multiple phases distinguished cross-cutting and abutting relationships among fractures, mineral sealing versus open fractures, and indicators of fault reactivation.

**1) Early Extensional Phase:** Characterized by the formation of open-mode extension joints and normal faults, notably the Nabhoi fault exhibiting a pure extensional stress regime, oriented NE-SW. This phase is identified by open fractures and absence of mineral sealing.

**2) Transtensive Phase Associated with Magmatic Intrusions:** Marked by the development of en-echelon shear fractures, veins, and strike-slip to oblique-slip faults, including the N-S to NNE-SSW oriented faults near the Nanamo Hill plug and KHF. Mineral sealing in veins and sealed joints indicates multiple deformation events, while open fractures and cross-cutting relationships show ongoing activity. Paleostress analysis links this phase to a transtensive regime with evolving stress orientations from N-S to NNE-SSW.

**3) Reactivation and Transpressive Phase:** Evidenced by reactivation of older

faults (faults near KHF) showing compressive or transpressive stress patterns, with features such as pinnet joints and antithetic faults forming along strike-slip faults. Cross-cutting relationships and overprinting of fracture sets indicate this later phase under a transpressive regime with maximum compression from NNW-SSE and NW-SE.

Each phase is temporally constrained by the relative timing of fault and fracture generations, mineralization stages, and structural overprints, correlating with the transition from pure extension (Nabhoi fault) to transtension linked with magmatic activity, and finally to transpression during fault reactivation.

## 8. Conclusions

- The western segment of the Katrol Hill Fault (KHF) has a complex deformation history characterized by multiple generations of faults, joints and fault-related folds. The analysis indicates that the tectonic stress fields in the region were not static, leading to progressive fracturing of the rock masses over time. This is evidenced by the presence of various fracture types, such as open-mode extension fractures, veins and sealed joints, which, despite sharing an N-S orientation, likely formed during different deformation events.
- Structural and fracture analyses of the western segment of the Katrol Hill Fault (KHF) and its surrounding region revealed a complex interplay of faulting, folding and fracture development influenced by multiple deformation events.
- The KHF exhibits an east-west to ENE-WSW/ESE-WNW-trending fault system characterized by moderate to steeply dipping asymmetric flexures and a network of strike-slip and oblique-slip faults that dissect the fault zone.
- The presence of various fracture types, including extension joints, veins, en-echelon shear fractures and pinnet joints, indicates multiple phases of deformation under varying stress regimes.
- Paleostress reconstructions suggest a transtensive stress regime with N-S to NNE-SSW orientations linked to magmatic intrusions, such as the Nanamo Hill plug and KHF activity.
- The faults in the area are predominantly oblique-slip, with some normal and strike-slip faults. Paleo-stress analysis suggests that stress conditions changed over time, causing the generation of new faults and reactivation of older ones. For instance, faults near the KHF show signs of reactivation with different stress patterns (compressive or transpressive) along the fault planes. The Nabhoi fault, a major normal fault in the south, exhibits a pure extensional stress field and appears to be older than or synchronous with other faults, as it is cross-cut and displaced by a younger NNE-SSE fault.
- Fault-related folds are prominent along the KHF and Nabhoi faults. The KHF displays both normal and reverse drag folds along its length, a phenomenon dependent on the orientation of rock layers relative to the fault and the dominance of fault-parallel versus fault-normal displacement. The Nabhoi fault

features a reverse-drag anticline on its hanging wall and a synclinal basin on its footwall. Conical drag folds, such as the anticline at the western end of the Nabhoi fault, formed owing to the passive rotation of competent rock layers within softer flowing media near fault intersections.

- Fault-related folds, including normal and reverse drag folds, demonstrate heterogeneous displacement fields along faults, with fold geometries influenced by fault-parallel and fault-normal displacement components. The development of conical drag folds and associated brecciation further highlights the mechanical heterogeneity of the lithologies and the dynamic nature of fault deformation.
- These structural features, including the Waramseda nose, Gurukul Dungar anticline, and folds along the Nabhoi fault, collectively form a structural basin between the KHF and Nabhoi fault. This basin was subsequently filled with sediments, forming the Kurbai plant bed, which was gently folded by the ongoing, progressive deformation of the KHF.
- Overall, this study emphasizes the significance of integrating field observations, remote sensing and paleostress analysis to elucidate the deformation history and kinematic evolution of the KHF and adjacent structures.
- These findings contribute to a better understanding of fault segmentation and fracture network development in the Kachchh Rift Basin.

## Acknowledgements

Babulal Vaghela is thankful to the Department of Geosciences, Kachchh University, and R. R. Lalan College for their technical support. Jigar Joshi, Dheer Kundaliya, Kanti Goradiya and Mohan Jajani for their support during the field visits.

## Conflicts of Interest

The authors declare no conflicts of interest regarding the publication of this paper.

## References

- [1] Kim, Y., Peacock, D.C.P. and Sanderson, D.J. (2004) Fault Damage Zones. *Journal of Structural Geology*, **26**, 503-517. <https://doi.org/10.1016/j.jsg.2003.08.002>
- [2] Fialko, Y., Sandwell, D., Agnew, D., Simons, M., Shearer, P. and Minster, B. (2002) Deformation on Nearby Faults Induced by the 1999 Hector Mine Earthquake. *Science*, **297**, 1858-1862. <https://doi.org/10.1126/science.1074671>
- [3] Hayward, K.S. and Cox, S.F. (2017) Melt Welding and Its Role in Fault Reactivation and Localization of Fracture Damage in Seismically Active Faults. *Journal of Geophysical Research: Solid Earth*, **122**, 9689-9713. <https://doi.org/10.1002/2017jb014903>
- [4] Viola, G., Scheiber, T., Fredin, O., Zwingmann, H., Margreth, A. and Knies, J. (2016) Deconvoluting Complex Structural Histories Archived in Brittle Fault Zones. *Nature Communications*, **7**, Article No. 13448. <https://doi.org/10.1038/ncomms13448>
- [5] Peacock, D.C.P., Sanderson, D.J. and Rotevatn, A. (2018) Relationships between

- Fractures. *Journal of Structural Geology*, **106**, 41-53.  
<https://doi.org/10.1016/j.jsg.2017.11.010>
- [6] Biswas, S.K. (2005) A Review of Structure and Tectonics of Kutch Basin, Western India, with Special Reference to Earthquakes. *Special Section: Intraplate Seismicity*, **88**, 1592-1600.
- [7] Biswas, S.K. (2016) Tectonic Framework, Structure and Tectonic Evolution of Kutch Basin, Western India. *Recent Studies on the Geology of Kachchh*, Kachchh, 1-24 August 2016, 129-150. <https://doi.org/10.17491/cgsi/2016/105417>
- [8] Biswas, S.K. (1987) Regional Tectonic Framework, Structure and Evolution of the Western Marginal Basins of India. *Tectonophysics*, **135**, 307-327.  
[https://doi.org/10.1016/0040-1951\(87\)90115-6](https://doi.org/10.1016/0040-1951(87)90115-6)
- [9] Thakkar, M.G., Mauryara, D.M., Raj, R. and Chamyal, L.S. (1999) Quaternary Tectonic History and Terrain Evolution of the Area around Bhuj, Mainland Kachchh, Western India. *Journal Geological Society of India*, **53**, 601-610.  
<https://doi.org/10.17491/jgsi/1999/530509>
- [10] Thakkar, M.G., Maurya, D.M., Rachna, R. and Chamyal, L.S., (2001) Morphotectonic Analysis of Khari Drainage Basin in Mainland Kachchh: Evidence for Neotectonic Activity along Transverse Faults. In: Gupta, L.N., Kumar, R. and Gill, G.S., Eds., *Structures and Tectonics of the Indian Plate*, IGA Special Publication, 205-220.
- [11] Maurya, D.M., Thakkar, M.G. and Chamyal, L.S. (2003) Implications of Transverse Fault System on Tectonic Evolution of Mainland Kachchh, Western India. *Current Science*, **85**, 661-667.
- [12] Sohoni, P.S. and Karanth, R.V. (2003) Jointing and Fracturing Characteristics of Central Kachchh Mainland, Kachchh, Western India. *Journal of the Geological Society of India*, **61**, 673-684. <https://doi.org/10.17491/jgsi/2003/610604>
- [13] Mallik, J. and Mathew, G. (2006) Structural Attributes of Major Faults in Kachchh, Western India: Seismotectonic Implications. *AGU Spring Meeting Abstracts*, Goa, 9-24 February 2006, T32A-01.
- [14] Mallik, J., Mathew, G., Angerer, T. and Greiling, R.O. (2008) Determination of Directions of Horizontal Principal Stress and Identification of Active Faults in Kachchh (India) by Electromagnetic Radiation (EMR). *Journal of Geodynamics*, **45**, 234-245.  
<https://doi.org/10.1016/j.jog.2008.01.003>
- [15] Kothiyari, G.C., Rastogi, B.K., Dumka, R.K. and Chauhan, G., (2015) Secondary Surface Deformation along the Bharudia/North Wagad Fault Zone in Kachchh Rift Basin, Western India. *Comunicações Geology*, **102**, 15-27.
- [16] Bhattacharya, F., Chauhan, G., Durga Prasad, A., Patel, R.C. and Thakkar, M.G. (2019) Strike-Slip Faults in an Intraplate Setting and Their Significance for Landform Evolution in the Kachchh Peninsula, Western India. *Geomorphology*, **328**, 118-137.  
<https://doi.org/10.1016/j.geomorph.2018.12.006>
- [17] Mishra, S., Kothiyari, G.C., Dubey, R.K. and Chauhan, G. (2021) Structural Attributes and Paleostress Analysis of Quaternary Landforms along the Vigodi Fault (VF) in Western Kachchh Region. *Quaternary International*, **599**, 210-222.  
<https://doi.org/10.1016/j.quaint.2020.07.038>
- [18] Shaikh, M., Maurya, D., Soumyajit, M., Vanik, N., Kumar, A. and Chamyal, L. (2020) Tectonic Evolution of the Seismically Active Western Continental Margin of the Indian Plate: Implications for Kinematic History and Fluid Flow. *22nd EGU General Assembly*, 4-8 May 2020, Vol. 140, Article 104124.
- [19] Shaikh, M.A., Maurya, D.M., Mukherjee, S., Vanik, N.P., Padmalal, A. and Chamyal,

- L.S. (2020) Tectonic Evolution of the Intra-Uplift Vigodi-Gugriana-Khirsara-Netra Fault System in the Seismically Active Kachchh Rift Basin, India: Implications for the Western Continental Margin of the Indian Plate. *Journal of Structural Geology*, **140**, Article ID: 104124. <https://doi.org/10.1016/j.jsg.2020.104124>
- [20] Jani, C., Kandregula, R.S., Bhosale, S., Chavan, A., Lakhote, A., Bhandari, S., *et al.* (2021) Delineation of Tectonically Active Zones in the Island Belt Uplift Region, Kachchh Basin, Western India: A Geomorphic and Geodetic Approach. *Quaternary Science Advances*, **4**, Article ID: 100034. <https://doi.org/10.1016/j.qsa.2021.100034>
- [21] Biswas, S.K. (1993) *Geology of Kutch*. K. D. Malaviya Institute of Petroleum Exploration, 450 p.
- [22] Kothiyari, G.C., Dumka, R.K., Singh, A.P., Chauhan, G., Thakkar, M.G. and Biswas, S.K. (2016) Tectonic Evolution and Stress Pattern of South Wagad Fault at the Kachchh Rift Basin in Western India. *Geological Magazine*, **154**, 875-887. <https://doi.org/10.1017/s0016756816000509>
- [23] Sohoni, P.S., Malik, J.N., Merh, S.S. and Karanth, R.V. (1999) Active Tectonics Across Katrol Hill Zone, Kachchh, Western India. *Journal Geological Society of India*, **53**, 579-586. <https://doi.org/10.17491/jgsi/1999/530506>
- [24] Maurya, D.M., Chowksey, V., Tiwari, P. and Chamyal, L.S. (2017) Tectonic Geomorphology and Neotectonic Setting of the Seismically Active South Wagad Fault (SWF), Western India, Using Field and GPR Data. *Acta Geophysica*, **65**, 1167-1184. <https://doi.org/10.1007/s11600-017-0099-5>
- [25] Patidar, A.K., Maurya, D.M., Thakkar, M.G. and Chamyal, L.S. (2007) Fluvial Geomorphology and Neotectonic Activity Based on Field and GPR Data, Katrol Hill Range, Kachchh, Western India. *Quaternary International*, **159**, 74-92. <https://doi.org/10.1016/j.quaint.2006.08.013>
- [26] Patidar, A.K., Maurya, D.M., Thakkar, M.G. and Chamyal, L.S. (2008) Evidence of Neotectonic Reactivation of the Katrol Hill Fault during Late Quaternary and Its GPR Characterization. *Current Science*, **94**, 338-346. <http://www.jstor.org/stable/24100341>
- [27] Bhattacharya, F., Rastogi, B.K., Ngangom, M., Thakkar, M.G. and Patel, R.C. (2013) Late Quaternary Climate and Seismicity in the Katrol Hill Range, Kachchh, Western India. *Journal of Asian Earth Sciences*, **73**, 114-120. <https://doi.org/10.1016/j.jseaes.2013.04.030>
- [28] Das, A., Chauhan, G., Prizomwala, S.P., Thakkar, M.G. and Rastogi, B.K. (2016) Tectonic Variability along the South Katrol Hill Fault, Kachchh, Western India: Insights from Geomorphic Indices. *Zeitschrift für Geomorphologie*, **60**, 209-218. <https://doi.org/10.1127/zfg/2016/0201>
- [29] Das, A., Prizomwala, S.P., Solanki, T., Chauhan, G., Thakkar, M.G. and Bhatt, N. (2019) Relative Assessment of Tectonic Activity along the Seismically Active Katrol Hill Fault, Kachchh, Western India. *Journal of the Geological Society of India*, **94**, 179-187. <https://doi.org/10.1007/s12594-019-1287-5>
- [30] Talati, R.N. (2018) Occurrence of Fibrous Calcite in Miliolite Limestone of the Katrol Hill Range, Kachchh, Western India: New Evidence of Tectonic Activity along the KHF. *International Journal of Emerging Trends in Science and Technology*, **5**, 6732-6736. <https://doi.org/10.18535/ijetst/v5i9.02>
- [31] Tiwari, P., Maurya, D.M., Shaikh, M., Patidar, A.K., Vanik, N., Padmalal, A., *et al.* (2021) Surface Trace of the Active Katrol Hill Fault and Estimation of Paleo-Earthquake Magnitude for Seismic Hazard, Western India. *Engineering Geology*, **295**, Article ID: 106416. <https://doi.org/10.1016/j.enggeo.2021.106416>

- [32] Biswas, S.K. (2016) Mesozoic and Tertiary Stratigraphy of Kutch\* (Kachchh)? A Review. In: Thakkar, M.G., Ed., *Recent Studies on the Geology of Kachchh*, Geological Society of India, Special Publication 6, 1-24.  
<https://doi.org/10.17491/cgsi/2016/105405>
- [33] Biswas, S.K. and Deshpande, S.V. (1970) Geological and Tectonic Maps of Kutch. ONGC Bulletin, Vol. 7, 115-116.
- [34] Lageson, D.R., Larsen, M.C., Lynn, H.B. and Treadway, W.A. (2012) Applications of Google Earth Pro to Fracture and Fault Studies of Laramide Anticlines in the Rocky Mountain Foreland. In: Whitmeyer, S.J., Bailey, J.E., De Paor, D.G. and Ornduff, T., Eds., *Google Earth and Virtual Visualizations in Geoscience Education and Research*, Geological Society of America, 209-220. [https://doi.org/10.1130/2012.2492\(15\)](https://doi.org/10.1130/2012.2492(15))
- [35] Delvaux, D. and Sperner, B. (2003) New Aspects of Tectonic Stress Inversion with Reference to the TENSOR Program. *Geological Society, London, Special Publications*, **212**, 75-100. <https://doi.org/10.1144/gsl.sp.2003.212.01.06>
- [36] Angelier, J. (1994) Fault Slip Analysis and Paleostress Reconstruction. In: Hancock, P.L., Ed, *Continental Deformation*, Pergamon Press, 53-101.
- [37] Delvaux, D., Moeys, R., Stapel, G., Petit, C., Levi, K., Miroshnichenko, A., *et al.* (1997) Paleostress Reconstructions and Geodynamics of the Baikal Region, Central Asia, Part 2. Cenozoic Rifting. *Tectonophysics*, **282**, 1-38.  
[https://doi.org/10.1016/s0040-1951\(97\)00210-2](https://doi.org/10.1016/s0040-1951(97)00210-2)
- [38] Hancock, P.L. (1985) Brittle Microtectonics: Principles and Practice. *Journal of Structural Geology*, **7**, 437-457. [https://doi.org/10.1016/0191-8141\(85\)90048-3](https://doi.org/10.1016/0191-8141(85)90048-3)
- [39] Peacock, D.C.P. (2001) The Temporal Relationship between Joints and Faults. *Journal of Structural Geology*, **23**, 329-341.  
[https://doi.org/10.1016/s0191-8141\(00\)00099-7](https://doi.org/10.1016/s0191-8141(00)00099-7)
- [40] Grasemann, B., Martel, S. and Passchier, C. (2005) Reverse and Normal Drag along a Fault. *Journal of Structural Geology*, **27**, 999-1010.  
<https://doi.org/10.1016/j.jsg.2005.04.006>
- [41] Reches, Z. and Eidelman, A. (1995) Drag along faults. *Tectonophysics*, **247**, 145-156.  
[https://doi.org/10.1016/0040-1951\(94\)00170-e](https://doi.org/10.1016/0040-1951(94)00170-e)
- [42] Becker, A. (1995) Conical Drag Folds as Kinematic Indicators for Strike-Slip Fault Motion. *Journal of Structural Geology*, **17**, 1497-1506.  
[https://doi.org/10.1016/0191-8141\(95\)00057-k](https://doi.org/10.1016/0191-8141(95)00057-k)